ADVANCED MATERIALS INTERFACES
www.advmatinterfaces.de

Kinetics of Water Transfer Between the LCST and UCST Thermoresponsive Blocks in Diblock Copolymer Thin Films Monitored by In Situ Neutron Reflectivity

Neng Hu, Li Lin, Ezzeldin Metwalli, Lorenz Bießmann, Martine Philipp, Viet Hildebrand, Andre Laschewsky, Christine M. Papadakis, Robert Cubitt, Qi Zhong, and Peter Müller-Buschbaum**

The kinetics of water transfer between the lower critical solution temperature (LCST) and upper critical solution temperature (UCST) thermoresponsive blocks in about 10 nm thin films of a diblock copolymer is monitored by in situ neutron reflectivity. The UCST-exhibiting block in the copolymer consists of the zwitterionic poly(4-((3-methacrylamidopropyl)dimethylammonio) butane-1-sulfonate), abbreviated as PSBP. The LCST-exhibiting block consists of the nonionic poly(N-isopropylacrylamide), abbreviated as PNIPAM. The as-prepared $PSBP_{80}$-*b*-$PNIPAM_{400}$ films feature a three-layer structure, i.e., PNIPAM, mixed PNIPAM and PSBP, and PSBP. Both blocks have similar transition temperatures (TTs), namely around 32 °C for PNIPAM, and around 35 °C for PSBP, and with a two-step heating protocol (20 °C to 40 °C and 40 °C to 80 °C), both TTs are passed. The response to such a thermal stimulus turns out to be complex. Besides a three-step process (shrinkage, rearrangement, and reswelling), a continuous transfer of D_2O from the PNIPAM to the PSBP block is observed. Due to the existence of both, LCST and UCST blocks in the $PSBP_{80}$-*b*-$PNIPAM_{400}$ film, the water transfer from the contracting PNIPAM, and mixed layers to the expanding PSBP layer occurs. Thus, the hydration kinetics and thermal response differ markedly from a thermoresponsive polymer film with a single LCST transition.

1. Introduction

Thermoresponsive polymers are able to present rapid changes of their physical properties when exposed to thermal stimuli.[1,2] In general, two types of thermoresponsive behavior are encountered in aqueous solution: (1) Polymers exhibiting a lower critical solution temperature (LCST), and (2) polymers showing an upper critical solution temperature (UCST). In LCST type polymers, when the temperature is below the transition temperature (TT), the hydrophilic groups in the polymer chains tend to form strong intermolecular hydrogen bonds with water molecules. Thus, the polymers are in a highly hydrophilic state and able to swell. When the temperature is increased above the TT, the H-bonding to water molecules becomes weaker, and the polymer chains prefer to form intramolecular hydrogen bonds with neighboring chains. Hence, the previously formed intermolecular hydrogen

N. Hu, L. Lin,[+] Q. Zhong
Key Laboratory of Advanced Textile Materials and Manufacturing Technology
Ministry of Education
Zhejiang Sci-Tech University
Hangzhou 310018, China
E-mail: qi.zhong@zstu.edu.cn

The ORCID identification number(s) for the author(s) of this article can be found under https://doi.org/10.1002/admi.202201913.

[+]Present address: Lanxi Science and Technology Bureau, No. 500 Zhenxing Road, Lanxi 321100, China

[++]Present address: German University in Cairo – GUC, Faculty of Engineering and Materials Science (EMS), Materials Engineering Department, New Cairo City, Egypt

DOI: 10.1002/admi.202201913

E. Metwalli,[++] L. Bießmann, M. Philipp, Q. Zhong, P. Müller-Buschbaum
Technische Universität München
Physik-Department
Lehrstuhl für Funktionelle Materialien
James-Franck-Str. 1, 85748 Garching, Germany
E-mail: muellerb@ph.tum.de

V. Hildebrand, A. Laschewsky
Universität Potsdam
Institut für Chemie
Karl-Liebknecht-Str. 24–25, 14476 Potsdam-Golm, Germany

A. Laschewsky
Fraunhofer Institut für Angewandte Polymerforschung
Geiselbergstr. 69, 14476 Potsdam-Golm, Germany

C. M. Papadakis
Technische Universitat München
Physik-Department
Fachgebiet Physik Weicher Materie
James-Franck-Str. 1, 85748 Garching, Germany

R. Cubitt
Institut Laue-Langevin
6 rue Jules Horowitz, Grenoble 38000, France

P. Müller-Buschbaum
Heinz Maier-Leibnitz Zentrum (MLZ)
Technische Universität München
Lichtenbergstr. 1, 85748 Garching, Germany

bonds are broken and the water molecules are expelled, thus switching the polymer to a more hydrophobic state.[2,3] Poly(*N*-isopropylacrylamide), abbreviated as PNIPAM, is a typical and well investigated thermoresponsive polymer with LCST type behavior.[4] Its TT of ~32 °C makes PNIPAM also interesting for biological and medical applications.[5–7] In UCST type polymers, the transition behavior is reversed. Below the TT, they are water insoluble, but turn hydrophilic above the TT.[8,9] In case of zwitterionic polymers with UCST type, additional strong electrostatic forces are present.[10,11] As one of the zwitterionic polymers with UCST type, poly(sulfobetaine) finds much interest by virtue of a high biocompatibility[12–15] and is broadly applied in the fields of biology and medicine.[11,16–19] Importantly, apart from molecular variables such as the precise nature of the constitutional repeat unit or the molar mass,[3,20–23] the TT of poly(sulfobetaine) is strongly affected by various factors, such as the solution concentration and the presence of salt.[20–21,24–27]

Whereas thermoresponsive polymers with LCST type behavior were extensively studied in the last decade, fewer investigations focused on thermoresponsive polymers with UCST type behavior. Also copolymers containing both types of blocks, UCST and LCST type, were only studied to a limited extent.[28,29] At present, there is only little focus on the phase transitions of copolymers containing UCST and LCST type blocks in aqueous solution. The investigation demonstrated that micelles could show a "schizophrenic" aggregation behavior in aqueous solutions due to the existence of LCST and UCST type blocks in the copolymers.[16,30–32] Notably, so far little attention was also paid to the kinetic response of thin films prepared from thermoresponsive copolymers containing LCST and UCST type blocks.[33–36]

The kinetics of the thermal response of polymers in thin films differs from the solution behavior. Apart from the much higher volume fraction of the polymer in films, the presence of the solid support underneath the polymer film impacts the swelling and thermal response of the films due to the additional interactions between the substrate and the polymer.[37] Moreover, the polymer film's surface adds a second interface to the thin film system, which also needs to be considered with its interactions. In addition, unlike polymer chains in an aqueous solution,[38] which can be fully hydrated and freely move, in thin films the polymer chains are densely packed and relatively immobilized from each other. The polymer film is constrained between both interfaces and the solid substrate breaks the translational symmetry in thin films. Due to the restriction of polymer chain movement, not only the internal structure, but also the transition behavior of the thermoresponsive copolymer films containing both LCST and UCST type blocks are different from aqueous solutions.[38] Improving the understanding of the kinetics of thermoresponsive block copolymer films containing both LCST and UCST type blocks will be beneficial. In particular, since the LCST and UCST type blocks present opposite transition behaviors upon heating (the LCST block switches from a strongly hydrated state to a weakly one, whereas the UCST block behaves oppositely), a water transfer from the LCST to UCST type blocks might take place. By tailoring the molecular structure of the block copolymers as well as adjusting the molar mass of the LCST and UCST type blocks, so that both TTs are similar, a directional transfer of water from one block to the other block could occur in the film. Thereby, one block can act as a water reservoir for the other block, which is of interest for potential applications in biomedicine and smart sensors[39–42] as well as for photocatalytic water splitting.[43]

In this investigation, we focus on the evolution of the internal structure and the kinetics of the underlying water transfer in a thermoresponsive diblock copolymer film containing both UCST and LCST type blocks after applying a thermal stimulus. For the LCST-type block, we choose the well-known thermoresponsive polymer PNIPAM. For the UCST-type block, we select a poly(sulfobetaine), namely poly(4-(*N*-(3-methacrylamidopropyl)-*N*,*N*-dimethylammonio)butane-1-sulfonate), abbreviated as PSBP. The chemical structure of the block copolymer $PSBP_{80}$-*b*-$PNIPAM_{400}$ is displayed in **Figure 1**.

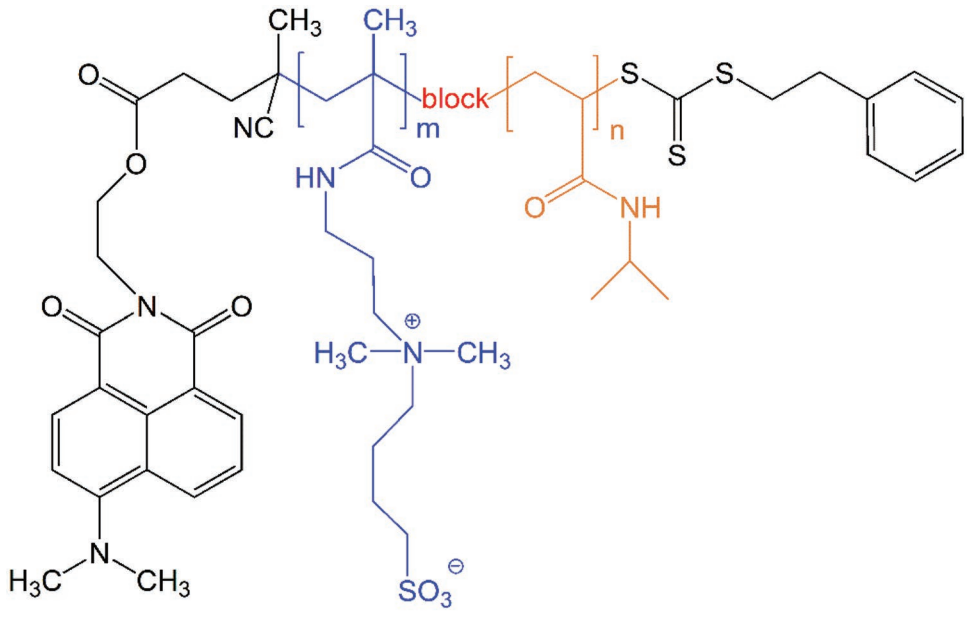

Figure 1. Chemical structure of the diblock copolymer $PSBP_m$-*b*-$PNIPAM_n$ in which $m = 80$ and $n = 400$.

To realize a high contrast between water and the studied diblock copolymer $PSBP_{80}$-*b*-$PNIPAM_{400}$ thin film, deuterated water (D_2O) is used in the in situ neutron reflectivity (in situ NR) measurements.[44] The degree of polymerization is 80 for PSBP and 400 for PNIPAM, so that the TT of the PNIPAM block is TT_{PNIPAM} = 32 °C. In the present investigation, the PSBP block features a pronounced transition when the temperature is increased from 20 °C to 40 °C. Due to the fact that TT_{PSBP} is somewhat higher than TT_{PNIPAM}, TT_{PSBP} can be assumed to be between 32 °C and 40 °C. Thus, both TTs are rather close to each other and with a two-step heating protocol (20 °C to 40 °C and 40 °C to 80 °C), we pass both TTs. Compared to the traditional approaches for structure information, in situ NR not only presents a good capability to probe the static structure vertical to the substrate, but also shows a high time resolution (5 s). Thus, the kinetic changes of thickness, roughness, and the content of D_2O in the interior of the film perpendicular to the film surface can be traced without any damage to the film.[45] The kinetics of water transfer can be well accessed by in situ NR and a diblock copolymer film is realized in which one block (PNIPAM) hydrates the other block (PSBP) upon heating.

2. Results and Discussion

2.1. Internal Structure Before Hydration

To well resolve the structural evolution of the $PSBP_{80}$-*b*-$PNIPAM_{400}$ thin film during hydration and after thermal stimuli, the internal structure before hydration is first probed by NR. After that, the kinetic change of the $PSBP_{80}$-*b*-$PNIPAM_{400}$ thin film in D_2O vapor atmosphere and upon heating is followed. The NR curve of the as-prepared $PSBP_{80}$-*b*-$PNIPAM_{400}$ thin film (**Figure 2**a) shows pronounced Kiessig fringes in the intensity, indicating that the as-prepared copolymer film is homogenous and has a smooth surface. The NR curve is well fitted by a three-layer model (PNIPAM/mixed PNIPAM and PSBP/PSBP layers). From the fits, the thicknesses of PNIPAM, mixed PNIPAM and PSBP and PSBP layers are determined as 54 ± 2, 50 ± 2, and 10 ± 1 Å, respectively. Thus, the total copolymer film thickness is 114 ± 2 Å. The corresponding scattering length density (SLD) profile is seen in Figure 2b. The SLD values of the three layers are (0.84 ± 0.02) × 10^{-6} $Å^{-2}$ (PNIPAM-rich layer), (0.77 ± 0.02) × 10^{-6} $Å^{-2}$ (mixed PNIPAM and PSBP layer), and (0.68 ± 0.02) × 10^{-6} $Å^{-2}$ (PSBP-rich layer). Thus, the SLD values of the PNIPAM layer and PSBP layer are slightly smaller than their respective theoretical values (0.87 × 10^{-6} and 0.73 × 10^{-6} $Å^{-2}$), which is attributed to the absorption of moisture by the polymer, as reported previously.[46] Based on the SLD values of H_2O, PSBP and PNIPAM, the initial volume fraction of H_2O in the PSBP layer and PNIPAM layer is calculated as 3.8% and 3.2%, respectively. According to the SLD value of PSBP, PNIPAM and the mixed layer (0.77 × 10^{-6} $Å^{-2}$), the molar ratio of PNIPAM and PSBP in the mixed layer is calculated as 1.3:1.0.

2.2. Hydration Kinetics in D_2O Vapor Atmosphere

The evolution of the internal structure and kinetics of hydration of the $PSBP_{80}$-*b*-$PNIPAM_{400}$ thin film are studied with in situ NR in D_2O vapor at 20 °C. As shown in **Figure 3**a, the number of Kiessig fringes in the probed q_z range increases from the beginning (bottom) to the end (top) of the hydration. This change illustrates the swelling of the copolymer film takes place by the absorption of D_2O.

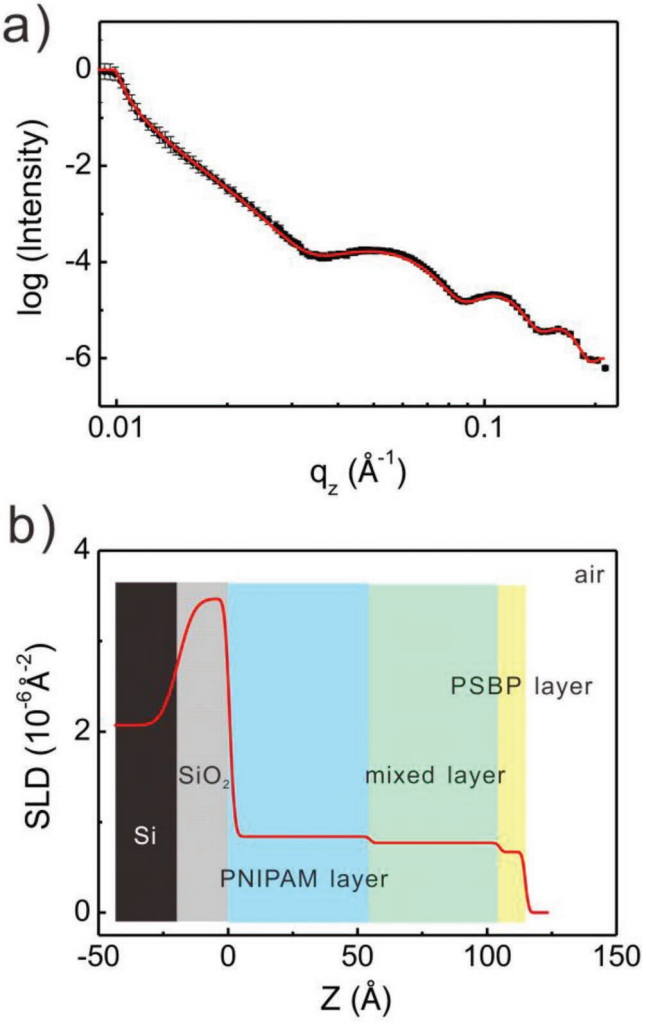

Figure 2. a) Neutron reflectivity (NR) data of the as-prepared $PSBP_{80}$-*b*-$PNIPAM_{400}$ film (black dots) shown together with the model fit (red line). q_z is defined as the scattering vector component in *z* direction. b) Resulting scattering length density (SLD) profile along the surface normal (*Z*-axis) of the film with $Z = 0$ indicating the top surface of the silicon oxide (SiO_2) layer. Si (black), SiO_2 (gray), PNIPAM (blue), mixed (green), and PSBP (yellow) layers are highlighted in the SLD profile.

By applying the three-layer fit model (PNIPAM/mixed PNIPAM and PSBP/PSBP), the initial stage of hydration (before 115 s) of the $PSBP_{80}$-*b*-$PNIPAM_{400}$ thin film can be well fitted. After that, an additional D_2O enrichment layer, located above the SiO_2 layer, is required to improve the fits. This enrichment layer is attributed to the attraction of D_2O by the hydrophilic substrate. A similar behavior was observed in previous investigations about the hydration of thermoresponsive polymer films with single LCST type behavior.[44] More structural details, such as film thickness and SLD profile, can be derived from the model fit. As presented in Figure 3b, pronounced differences

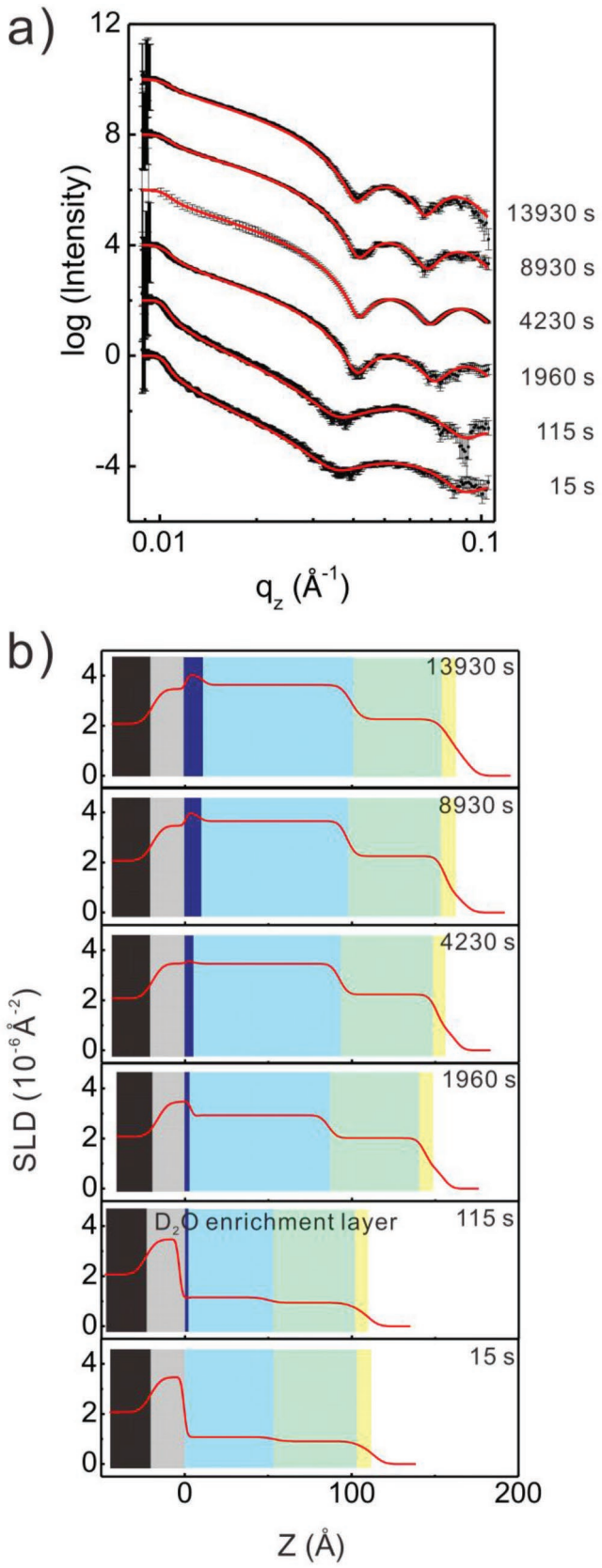

between the PNIPAM (LCST type) and the PSBP (UCST type) layers are observed during the hydration. For the latter almost no change is observed. The PSBP layer thickness remains unchanged and its SLD value slightly increases from 0.68×10^{-6} to 0.80×10^{-6} Å^{-2}. This behavior is caused by the occupation of the free volume in the PSBP by D_2O molecules.[47] In contrast, with the progress of hydration, the thicknesses of the PNIPAM layer and the mixed layer increase. Moreover, a D_2O enrichment layer emerges above the SiO_2 layer (marked in dark blue in Figure 3b). When the hydration reaches the equilibrium state, the thickness and SLD value of D_2O enrichment layer are 10 ± 1 and 4.05×10^{-6} Å^{-2}, respectively. Because the mixed layer contains largely PNIPAM, the fully hydrated mixed layer reaches a thickness of 59 ± 2 Å, whereas the SLD value is 2.26×10^{-6} Å^{-2} at 20 °C. The hydration of the pure PNIPAM layer is even more pronounced. Its thickness increases from 54 ± 2 to 89 ± 2 Å, while the SLD value rises from 0.84×10^{-6} to 3.63×10^{-6} Å^{-2}.

The D_2O volume fraction $\varphi(D_2O)$ in the hydrated $PSBP_{80}$-*b*-$PNIPAM_{400}$ film can be calculated via

$$\varphi(D_2O) = \frac{SLD_{layer} - SLD_0}{SLD_{D_2O} - SLD_0} \times 100\% \quad (1)$$

in which SLD_{layer} is the SLD value of each layer obtained from the model fit. SLD_0 and SLD_{D2O} are the SLD values of each layer in the as-prepared $PSBP_{80}$-*b*-$PNIPAM_{400}$ film and D_2O, respectively. Therefrom, the total amount of $\varphi(D_2O)$ in the film can be obtained by Equation (2):

$$\varphi(D_2O) = \sum_{Z=1}^{4} \varphi(D_2O)_Z \times V_Z \quad (2)$$

In which $\varphi(D_2O)_z$ and V_Z indicate the volume fraction of D_2O in each layer and the volume fraction of the corresponding layer.

As shown in **Figure 4**a, the evolution of film thickness for the $PSBP_{80}$-*b*-$PNIPAM_{400}$ thin film in D_2O vapor can be divided into two stages, which is very different from that of $\varphi(D_2O)$ (Figure 4a). In the first stage, from 15 s (i.e., 15 s after the injection of D_2O) to 115 s, the D_2O volume fraction $\varphi(D_2O)$ significantly rises from $2.7 \pm 0.8\%$ to $5.2 \pm 0.8\%$. In contrast, the normalized film thickness $d_{hydr}/d_{as\text{-}prep}$ increases only slightly from 1.00 ± 0.02 to 1.02 ± 0.02. A similar hydration behavior was reported before and attributed to the occupation of the free volume.[44,48] Thus, also in the initial water uptake step of the $PSBP_{80}$-*b*-$PNIPAM_{400}$ thin film, its free volume is filled by D_2O molecules so that the film thickness almost remains unchanged

Figure 3. Hydration kinetics of the as-prepared $PSBP_{80}$-*b*-$PNIPAM_{400}$ film in D_2O vapor atmosphere at 20 °C. a) Six selected neutron reflectivity (NR) curves (black dots) shown together with model fits (red lines). b) Resulting scattering length density (SLD) profiles normal to the surface of the $PSBP_{80}$-*b*-$PNIPAM_{400}$ film. The position Z = 0 Å indicates the top surface of the silicon oxide (SiO_2) layer. Si (black), SiO_2 (gray), D_2O enrichment (dark blue), PNIPAM (blue), mixed (green), and PSBP (yellow) layers are highlighted in the SLD profiles.

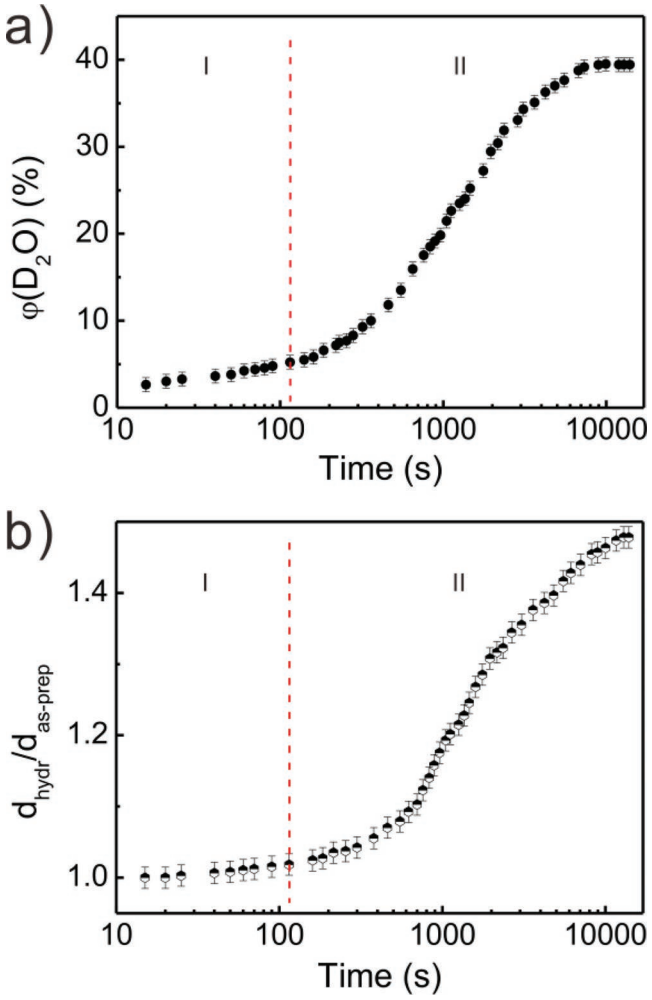

Figure 4. Hydration kinetics of $PSBP_{80}$-*b*-$PNIPAM_{400}$ thin film in a D_2O vapor atmosphere at 20 °C. a) $\varphi(D_2O)$ and b) $d_{hydr}/d_{as\text{-}prep}$ of the entire film. The hydration process is divided into two stages by the red dashed lines and indicated by Roman letters (I and II) in the graphs.

while $\varphi(D_2O)$ strongly increases. Thereby, the chain mobility of the copolymer is increased. After that, $\varphi(D_2O)$ increases dramatically from 5.2 ± 0.8% to 39.6 ± 0.8% in the second stage of hydration. Simultaneously, $d_{hydr}/d_{as\text{-}prep}$ pronouncedly increases from 1.02 ± 0.02 to 1.48 ± 0.02.

More details about the hydration are gained from the behavior of the individual layers. The individual water uptake is shown in **Figure 5**. $\varphi(D_2O)$ in the PSBP layer only presents a minor increase to 2.3 ± 0.1% without changing the thickness. This is attributed to the occupation of the free volume in the PSBP layer by D_2O. In comparison, the mixed PNIPAM and PSBP layer is able to absorb a larger amount of D_2O at 20 °C due to the large PNIPAM content in this layer. Thus, $\varphi(D_2O)$ in the mixed PNIPAM and PSBP layer increases to 26.4 ± 0.7%. An even more pronounced increase of $\varphi(D_2O)$ (from 3.8 ± 0.9% to 50.3 ± 0.9%) is observed for the pure PNIPAM layer, which is attributed to its high hydrophilicity at 20 °C. Based on the hydrophilic interaction between of PNIPAM layer and substrate, $\varphi(D_2O)$ of the formed D_2O enrichment layer can reach to 58.5 ± 0.5%.

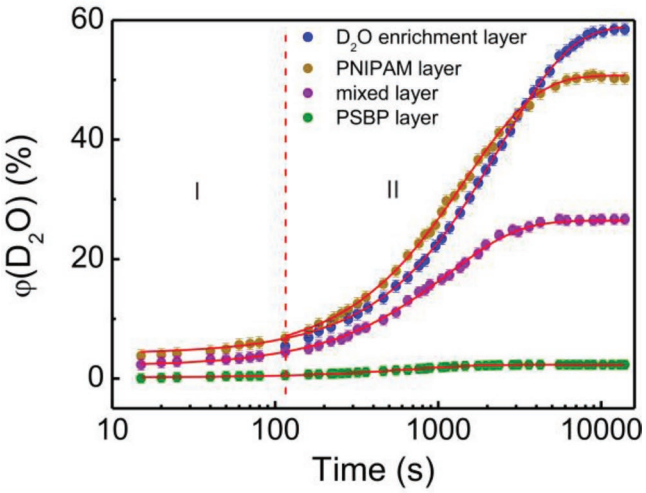

Figure 5. Time-dependent $\varphi(D_2O)$ in the individual layers during the hydration process in D_2O vapor atmosphere at 20 °C: PSBP (green), mixed (purple), PNIPAM (brown), and D_2O (blue) enrichment layers. The hydration process is divided into two stages by the red dashed lines and indicated by Roman letters (I and II) in the graph.

According to our former experience, the kinetics of the hydration process of thermoresponsive polymer thin films can be well described by a diffusion model from Li and Tanaka[37,47,49]

$$\ln\left(\frac{\varphi(D_2O)_\infty - \varphi(D_2O)}{\varphi(D_2O)_\infty}\right) = \ln B - \frac{t}{\tau} \quad (3)$$

in which $\varphi(D_2O)_\infty$ and $\varphi(D_2O)$ are the volume fractions of D_2O absorbed at infinite time and time t (the equilibrium state), respectively. B and τ are a constant and the relaxation time, respectively. The fit parameters obtained for these four sublayers are presented in Table S1 (Supporting Information). The relaxation time τ of the D_2O enrichment layer is much longer than those of the other layers, which is consistent with our previous investigation.[37] It is also related to the hydrophilicity of SiO_2 layer. Whereas the values of constant B in all these four layers are the same if considering the fit error.

2.3. Kinetic Response Triggered by First-Stage Thermal Stimulus

To investigate the water transfer between the PSBP and PNIPAM blocks in $PSBP_{80}$-*b*-$PNIPAM_{400}$ thin film during the phase transition, two thermal stimuli are applied: In the first step, the temperature is rapidly increased from 20 °C to 40 °C (first thermal stimulus). Because 40 °C is higher than the TTs of both blocks, the PNIPAM block turns to be less hydrophilic and expels D_2O, whereas the PSBP starts to become more hydrophilic and absorbs additional D_2O. In the second step, the temperature is rapidly increased further from 40 °C to 80 °C (second thermal stimulus). According to our previous investigation,[37,44,50] due to the interaction with the solid substrate, the thermoresponsive polymer thin films tend to show a much broader transition region compared to aqueous solutions. Also in the present study, both blocks (PNIPAM and

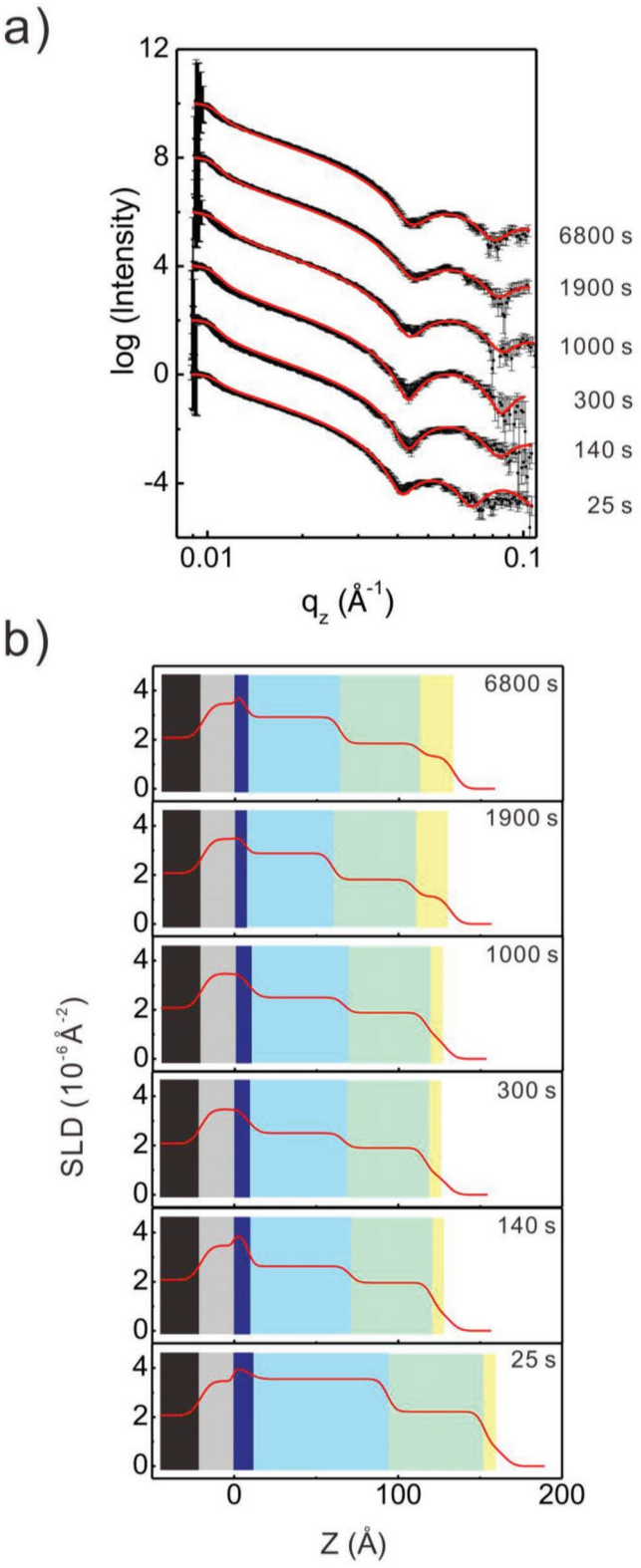

Figure 6. Kinetics of water transfer in the $PSBP_{80}$-*b*-$PNIPAM_{400}$ thin film after the first thermal stimulus (rapid increase of the temperature from 20 °C to 40 °C). a) Six selected neutron reflectivity (NR) curves (black dots) shown together with the model fits (red lines) from the beginning (bottom) to the end (top). The times marked in the graph are the corresponding time after the first thermal stimulus. b) Resulting scattering length density (SLD) profiles normal to the surface of the $PSBP_{80}$-*b*-$PNIPAM_{400}$ film. The position $Z = 0$ Å indicates the top surface of the silicon oxide (SiO_2) layer. The Si (black), SiO_2 (gray), D_2O enrichment (dark blue), PNIPAM (blue), mixed (green), and PSBP (yellow) layers are highlighted in the SLD profiles.

PSBP) show a broader transition region in the thin film format than in aqueous solution. Hence, the transition continues after the second thermal stimulus, and PNIPAM turns to be even less hydrophilic, while PSBP changes toward even more hydrophilic.

Six selected, exemplary NR curves from the beginning (bottom) to the end (top) of the first thermal stimulus are shown in **Figure 6**a. Interestingly, the intensity fringes first shift toward larger q_z values and then shift back toward lower q_z values. This behavior illustrates that the film first experiences a contraction, after which the film gradually reswells. To better understand the evolution of internal structure after the first thermal stimulus, the NR curves are fitted by the four-layer model mentioned above. As shown in Figure 6b, the thickness of the PNIPAM and mixed layers decrease sharply during the first 140 s. The thickness and the SLD value of the PNIPAM layer decrease from 84 ± 2 to 62 ± 2 Å and 3.60×10^{-6} to 2.61×10^{-6} Å^{-2}, respectively. In analogy, the thickness and SLD value of mixed layer slightly reduce from 59 ± 2 to 50 ± 2 Å and 2.25×10^{-6} to 1.92×10^{-6} Å^{-2}, respectively. The extent of shrinkage is smaller than in the pure PNIPAM layer due to the presence of PSBP in the mixed layer. In contrast, the PSBP layer becomes thicker with time. At the end of the first stimulus, the thickness and SLD value of the PSBP layer are 21 ± 2 and 1.33×10^{-6} Å^{-2}, respectively.

The behavior of the entire $PSBP_{80}$-*b*-$PNIPAM_{400}$ thin film during the first thermal stimulus (rapid increase of temperature from 20 °C to 40 °C) is shown in **Figure 7**. It is well described with three steps: shrinkage, rearrangement, and reswelling. In the first step, $\varphi(D_2O)$ pronouncedly reduces from 39.3 ± 0.4% to 24.2 ± 0.4% after 300 s (Figure 7a). Simultaneously $d/d_{\text{as-prep}}$ decreases from 1.44 ± 0.01 to 1.11 ± 0.01 (Figure 7b). This prominent shrinkage of the film thickness and expulsion of D_2O from the $PSBP_{80}$-*b*-$PNIPAM_{400}$ thin film can be attributed to the collapse of the well-hydrated PNIPAM blocks, which is triggered by the first thermal stimulus. In the second step, in the time range from 300 to 1000 s, both values of $\varphi(D_2O)$ and $d/d_{\text{as-prep}}$ are almost unchanged. In the third stage (from 1000 to 6800 s), $\varphi(D_2O)$ and $d/d_{\text{as-prep}}$ are increased from 23.4 ± 0.4% to 27.4 ± 0.4% and 1.10 ± 0.01 to 1.16 ± 0.01, respectively. Such an increase can be explained by the absorption of D_2O from the more hydrophilic PSBP block in the film. After that, both values remain almost unchanged. However, no direct information about a D_2O transfer between the PSBP and PNIPAM layers can be deduced from the evolutions of the entire film thickness and D_2O content.

Therefore, the evolution of $\varphi(D_2O)$ in the individual layers is further analyzed (**Figure 8**). As shown in Figure 8, the PSBP layer features a continuous uptake of D_2O after the first thermal stimulus. It is caused by the transition from a water insoluble to a more hydrophilic state when the temperature is pushed above the TT_{PSBP}.[51,52] In total, $\varphi(D_2O)$ in the PSBP

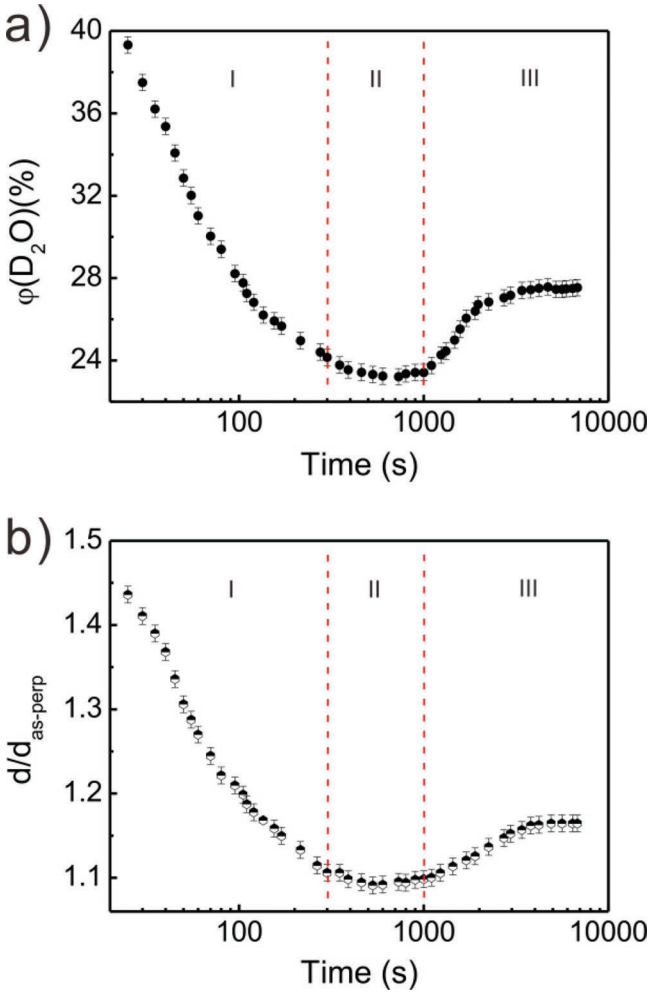

Figure 7. Evolution of a) $\varphi(D_2O)$ and b) $d/d_{as\text{-}prep}$ of the entire film after the first thermal stimulus (heating to 40 °C) applied to the $PSBP_{80}$-*b*-$PNIPAM_{400}$ thin film in a D_2O vapor atmosphere. The response after the first thermal stimulus is divided into three stages by the red dashed lines and indicated by Roman letters in the graphs.

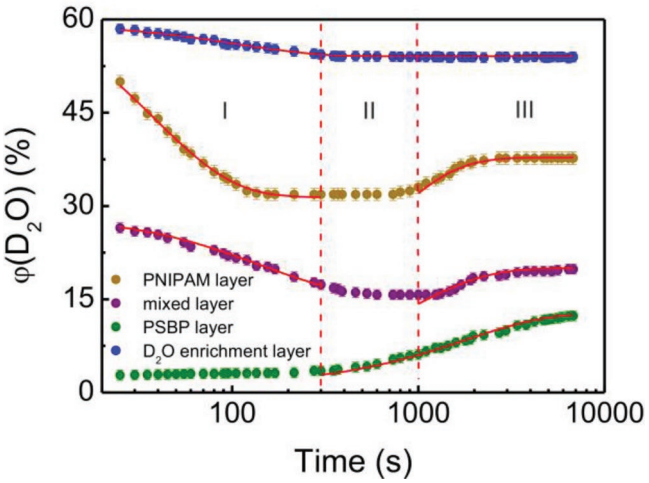

Figure 8. Evolution of $\varphi(D_2O)$ in the individual sublayers after the first thermal stimulus in D_2O vapor atmosphere: PSBP (green), mixed (purple), PNIPAM (brown), and D_2O enrichment (blue) layers. The solid lines are model fits as explained in the text. The response after the first thermal stimulus is divided into three stages by the red dashed lines and indicated by Roman letters (I and II) in the graph.

layer significantly rises from 2.8 ± 0.3% to 12.3 ± 0.3%. Because the water uptake rate is high, we assume that the D_2O, which is up-taken, comes directly from the PNIPAM and the mixed layers, instead of the absorption from the surrounding D_2O vapor atmosphere. D_2O expelled from these layers needs to pass the PSBP layer, which increases the chance of being taken up. In contrast, $\varphi(D_2O)$ in the PNIPAM layer behaves very differently. It exhibits three well distinguished kinetic regimes: (i) water release, (ii) constant water content, and (iii) water uptake. During the water release, $\varphi(D_2O)$ decreases from 50.0 ± 0.5% to 31.9 ± 0.5% (from 0 to 300 s). We attribute this behavior to the abrupt and pronounced phase transition of PNIPAM when the temperature increases above the TT_{PNIPAM}. Afterwards, $\varphi(D_2O)$ remains unchanged for 700 s (from 300 to 1000 s). Then, $\varphi(D_2O)$ gradually increases to 37.7 ± 0.5% in 6800 s. Such a minor reswelling behavior was already previously observed for PMDEGA- and PNIPMAM-based thermoresponsive polymer thin films.[44] It is attributed to the slow rearrangement of the collapsed polymer chains. Because the polymer chains are still in the D_2O vapor atmosphere, the chains are able to reabsorb the D_2O vapor during the chain arrangement. The mixed layer behaves very similarly to the PNIPAM layer. Again, three stages are observed which, however, are delayed versus the PNIPAM layer (from 0 to 300 s, from 300 to 1000 s and from 1000 to 6800 s). $\varphi(D_2O)$ in the mixed layer first reduces from 26.5 ± 0.4% to 17.4 ± 0.4%, remains constant, and then rises back to 19.9 ± 0.4% after the rearrangement regime. This similarity with the PNIPAM layer behavior is explained by the high PNIPAM content (volume fraction of about 60%) in the mixed layer, which dominates the overall transition. However, reduction and recovery are less pronounced than those in the PNIPAM layer, due to the presence of the PSBP component in the mixed layer. Thus, the opposite transition behavior of the PSBP layer also affects the total transition in the mixed layer. The D_2O enrichment layer simply presents a decrease in $\varphi(D_2O)$ from 58.5 ± 0.2% to 54.3 ± 0.2% with most of the water release occurring in the first 300 s, matching the temporal evolution of the water release from the mixed layer. This small change of $\varphi(D_2O)$ is caused by the attraction of D_2O by the hydrophilic SiO_2 layer, which hinders the transition of PNIPAM as well as the expulsion of D_2O from this layer. The evolution of the layer thicknesses is presented in Figure S1 (Supporting Information). Unlike the behavior of $\varphi(D_2O)$, no pronounced reswelling process of the PNIPAM layer is observed at the end of the first thermal stimulus. It might be related to the strong scattering of D_2O by neutrons, which causes the lower sensitivity of the layer thickness than that of $\varphi(D_2O)$ in the layer.

Similar to the hydration process, the behavior of the PNIPAM and mixed layers can be fitted by the model explained above. As shown in Table S2 (Supporting Information), the relaxation time for the chain collapse is much faster than that of the hydration process, illustrating that the shrinkage is more abrupt and pronounced. However, the constant *B* shows no difference for the collapse process.

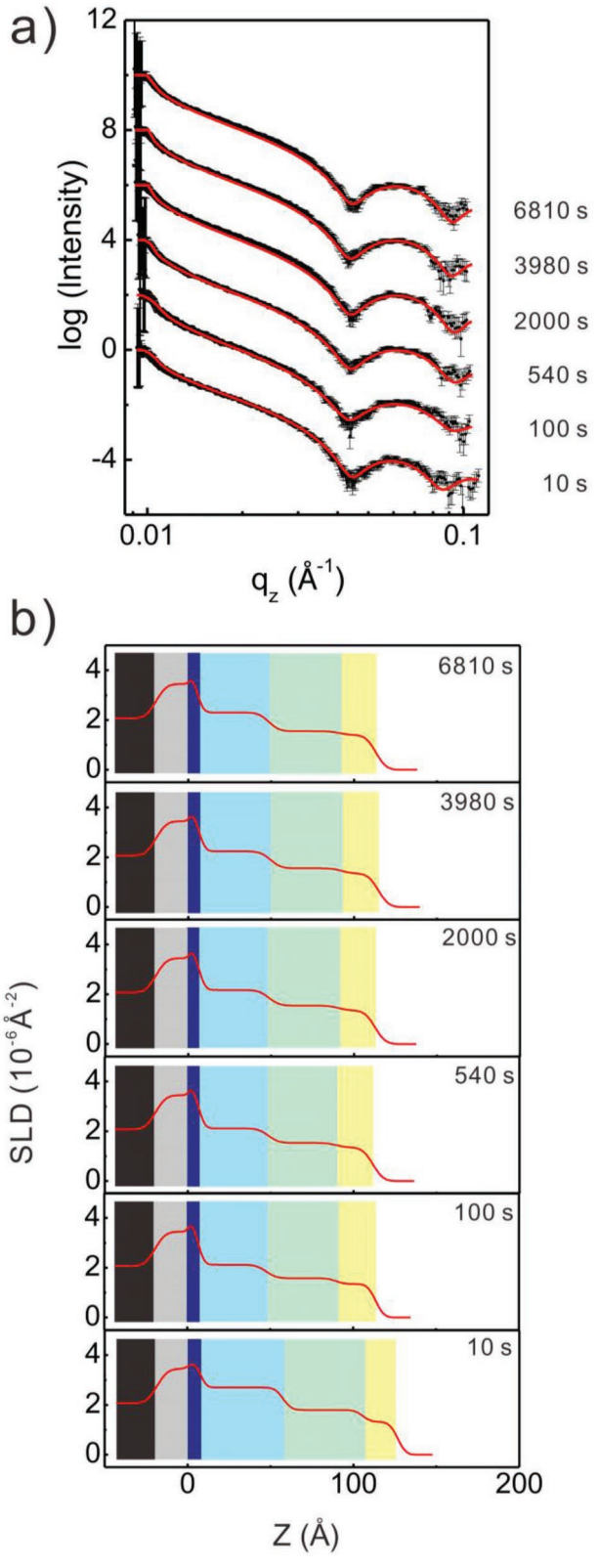

Figure 9. Kinetics of water transfer in the $PSBP_{80}$-*b*-$PNIPAM_{400}$ thin film after the second thermal stimulus (rapid increase of the temperature from 40 °C to 80 °C). a) Six selected neutron reflectivity (NR) curves (black dots) shown together with the model fits (red lines), b) resulting scattering length density (SLD) profiles normal to the surface of the $PSBP_{80}$-*b*-$PNIPAM_{400}$ film. The position $Z = 0$ Å indicates the top surface of the silicon oxide (SiO_2) layer. The Si (black), SiO_2 (gray), D_2O enrichment (dark blue), PNIPAM (blue), mixed (green), and PSBP (yellow) layers are highlighted in the SLD profiles.

2.4. Kinetic Response Triggered by Second-Stage Thermal Stimulus

The second thermal stimulus (rapid increase of temperature from 40 °C to 80 °C) is further applied to investigate the kinetic response of the copolymer film. **Figure 9**a shows six selected NR curves from the beginning (bottom) to the end (top) of the second thermal stimulus. First, the fringes in the NR curves shift toward higher q_z values, then almost remain unchanged and finally slightly shift toward lower q_z values. This indicates that the film first becomes thinner, and then almost remains constant in thickness. Again, all NR curves are well fitted by the four-layer model. The corresponding SLD profiles are presented in Figure 9b. Obvious changes happen only in the first 100 s due to a shrinkage of the PNIPAM and mixed layers. For more details, again the entire film behavior and that of the individual layers are inspected.

For the entire film, **Figure 10** shows the temporal evolution of $d/d_{\text{as-prep}}$ and $\varphi(D_2O)$ after the second thermal stimulus. Note that the final temperature is much higher than the TTs of PNIPAM and PSBP. For this reason, PNIPAM and PSBP feature more hydrophobic and more hydrophilic states, respectively, than at 40 °C. During the second thermal stimulus, the transition of the $PSBP_{80}$-*b*-$PNIPAM_{400}$ film still can be described by three stages, namely shrinkage, rearrangement, and reswelling (Figure 10a).[44] In the first stage (from 0 to 100 s), $\varphi(D_2O)$ decreases from 27.8 ± 0.5% to 19.8 ± 0.5%, while $d/d_{\text{as-prep}}$ also reduces from 1.13 ± 0.01 to 0.97 ± 0.01. Notably, the residual amount of D_2O is still substantial. In the second stage (from 100 to 2000 s), both $\varphi(D_2O)$ and $d/d_{\text{as-prep}}$ remain unchanged. In the third stage, $\varphi(D_2O)$ and $d/d_{\text{as-prep}}$ show a minor increase and slightly recover to 20.8 ± 0.5% and 0.99 ± 0.01, respectively. Thus, the final film thickness agrees with the initial film thickness within the uncertainty, despite a substantial amount of D_2O inside the film. Even in the minimum state, $\varphi(D_2O)$ in the film is still around 20.8 ± 0.2%. The residual water mainly contains two species: the first one is the water occupying the free volume in the film. Similar behavior was previously reported.[44] The second water species is retained by the now strongly hydrophilic PSBP block and the hydrophilic surface of the substrate.

To further investigate the details about the water content inside each part of the film, $\varphi(D_2O)$ is analyzed in each layer (**Figure 11**). $\varphi(D_2O)$ in the PSBP layer only slightly increases from 11.3 ± 0.5% to 12.9 ± 0.5%. This indicates that the second increase of temperature enhances the hydrophilicity of PSBP further. This increase happens basically in an abrupt step and can be correlated in part with the temporal evolution of $\varphi(D_2O)$ from the mixed layer (purple). This suggests that the expelled D_2O from the inner PNIPAM and mixed layers can be reabsorbed by PSBP layer. Concerning the PNIPAM layer, $\varphi(D_2O)$ decreases from 37.3 ± 0.3% to 23.0 ± 0.2% in the first stage (from 0 to 100 s) and then remains unchanged in the second stage

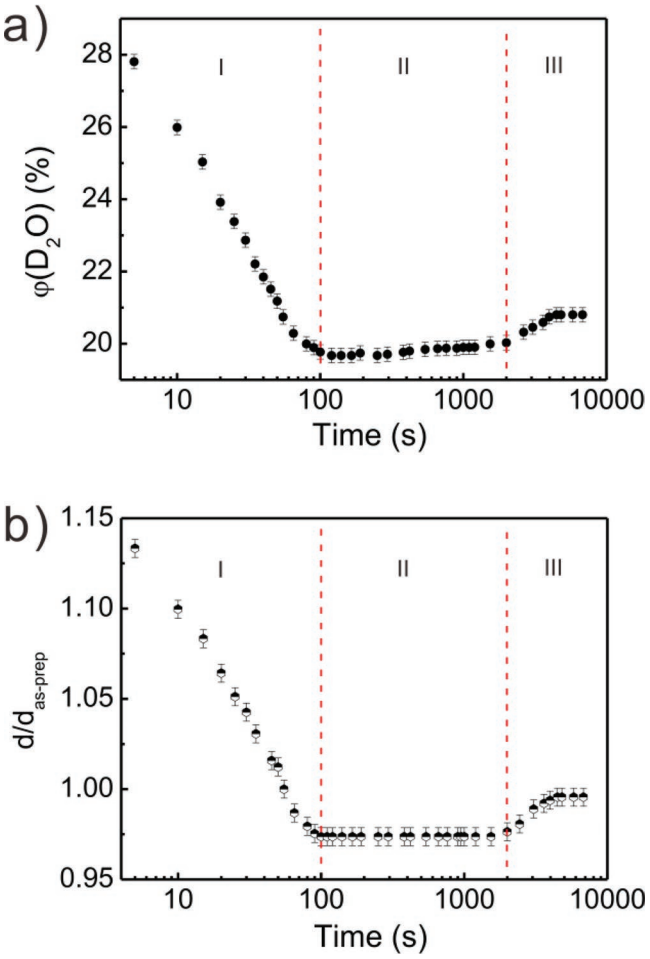

Figure 10. a) $\varphi(D_2O)$ and b) $d/d_{as\text{-}prep}$ of the entire film after the second thermal stimulus applied to the $PSBP_{80}$-*b*-$PNIPAM_{400}$ thin film in a D_2O vapor atmosphere. The response after the second thermal stimulus is divided into three stages by the red dashed lines and indicated by Roman letters in the graphs.

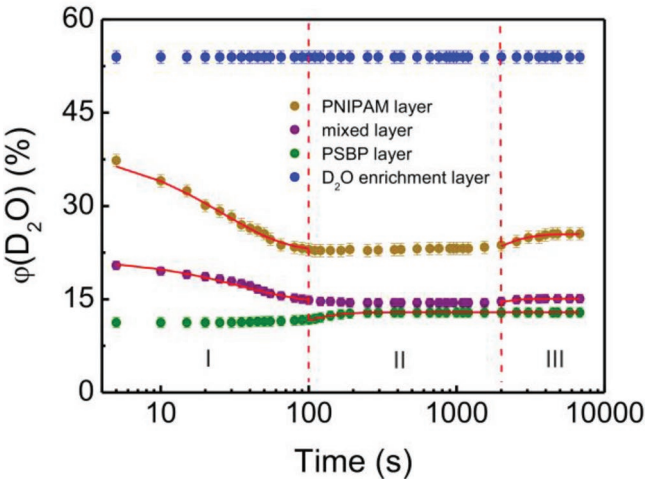

Figure 11. Evolution of $\varphi(D_2O)$ in the individual layers during the second thermal stimulus in D_2O vapor atmosphere: PSBP (green), mixed (purple), PNIPAM (brown), and D_2O enrichment (blue) layers. The red lines are model fits as explained in the text. The response after the second thermal stimulus is divided into three stages by the red dashed lines and indicated by Roman letters in the graph.

(from 100 to 2000 s). The contraction still can be described by the model of Li and Tanaka mentioned above. In addition, the relaxation time for the collapse is still short, i.e., the shrinkage of the PNIPAM chains is still fast (Table S3, Supporting Information). Surprisingly, even though the final temperature is well above TT_{PNIPAM}, the PNIPAM layer still undergoes a limited reswelling in the third stage (from 2000 to 6810 s). This unexpected reabsorption of D_2O can be explained by the quenching of the polymer chains after the thermal stimuli. Although the final temperature is well above the TT_{PNIPAM}, there is still a significant number of D_2O molecules inside the collapsed PNIPAM layer. This observation differs from our previous findings about the response behavior of PNIPAM homopolymer based thermoresponsive films. The presence of the hydrophilic PSBP block in the $PSBP_{80}$-*b*-$PNIPAM_{400}$ film is most likely the reason which causes the differences. Therefore, the rearranged chains can slowly reabsorb D_2O with time. The mixed layer (purple) shows a similar behavior concerning $\varphi(D_2O)$ as the PNIPAM layer. Only the extents of the contraction and reswelling processes are weaker. Interestingly, $\varphi(D_2O)$ in the D_2O enrichment layer remains constant (54.0 ± 0.5%) during the entire process. Thus, the highly hydrophilic SiO_2 layer established by the applied substrate cleaning protocol favors the formation of an ultrathin water film irrespective of the temperature, which is virtually not affected by the polymer coating on top.

3. Conclusion

The water uptake and temperature-dependent evolution of the internal structure and the kinetics of water transfer in a thin film of the thermoresponsive diblock copolymer $PSBP_{80}$-*b*-$PNIPAM_{400}$ are investigated in detail by in situ NR. Due to the presence of two thermoresponsive blocks with an LCST type (PNIPAM) and a USCT type (PSBP) behavior, the response to a thermal stimulus turns out to be complex. The as-prepared film shows a three-layer substructure (PSBP/mixed PSBP and PNIPAM/PNIPAM). After being exposed to an unsaturated D_2O vapor atmosphere at 20 °C an additional D_2O enrichment layer is formed at the SiO_2-polymer interface due to the strong attraction of D_2O by the hydrophilic substrate. Moreover, only the layers containing PNIPAM blocks (i.e., the PNIPAM and the mixed layer) absorb D_2O and swell. Almost no water absorption is observed in the zwitterionic PSBP layer, when the temperature is below the TT_{PSBP}. After the first thermal stimulus (temperature rapidly increased from 20 °C to 40 °C), a complicated three-step process (shrinkage, rearrangement, and reswelling) is observed for the PNIPAM and mixed layers. Their different time constants contribute to an even higher degree of complexity in the behavior of the entire film. From the three steps, the most pronounced one is the expulsion of D_2O from the PNIPAM layer due to the coil-to-globule collapse of the previously extensively hydrated PNIPAM chains. The mixed layer presents a similar collapse behavior as the PNIPAM layer after

the first thermal stimulus, though weaker in time, which can be explained by its high PNIPAM content (volume fraction of ≈60%). Interestingly, an immediate increase of D_2O is observed in the PSBP layer after the first thermal stimulus, which can be attributed to the water transfer from the contracting PNIPAM and mixed layers to the expanding PSBP layer. An expulsion of D_2O from the D_2O enrichment layer is not detected, most probably due to the strong attraction of D_2O to the hydrophilic substrate surface. Because PSBP switches to a more hydrophilic state at elevated temperatures, the amount of absorbed D_2O continues to increase in the PSBP layer with an increased time. After the second thermal stimulus (temperature rapidly increased from 40 °C to 80 °C), the behavior of the individual layers closely resembles that observed after the first thermal stimulus. Surprisingly, although the final temperature is well above the TT_{PNIPAM}, a certain amount of D_2O is still retained in the PNIPAM and mixed layers. This difference to the observations for PNIPAM homopolymer films can be caused by the proximity of PNIPAM to the PSBP block, which is strongly hydrophilic at elevated temperatures. It underlines, that copolymer films combining blocks with UCST and LCST type behaviors feature an enhanced level of complexity compared to the underlying homopolymers when exposed to humidity or thermal stimuli. Although the final temperature is well above the TT_{PNIPAM}, a significant larger amount of D_2O molecules still remains inside the collapsed PNIPAM layer. This observation differs from our previous findings about the response behavior of PNIPAM homopolymer based thermoresponsive thin films. Therefore, it can be concluded that the presence of the UCST type PSBP block profoundly influences the thermal response and final state of the $PSBP_{80}$-*b*-$PNIPAM_{400}$ thin films at high temperature.

4. Experimental Section

The details for the materials, substrate cleaning, thin film preparation, and the in situ NR measurements can be found in the Supporting Information.

Materials and Film Preparation: Diblock copolymer $PSBP_{80}$-*b*-$PNIPAM_{400}$ was synthesized by sequential reversible deactivation radical polymerizations adapting an established protocol.[53] The details about the materials, substrate cleaning details, and thin film preparation protocol are provided in the Supporting Information. The used silicon (Si) substrate had a hydrophilic silicon oxide layer (SiO_2, 20 ± 2 Å). Thin $PSBP_{80}$-*b*-$PNIPAM_{400}$ films were spin coated from trifluoroethanol solution and had a thickness of 114 ± 2 Å (error determined from the model fits).

In Situ NR Measurements: The in situ NR measurements were performed at the D17 reflectometer in ILL (Grenoble, France).[37] Instrument settings are provided in the Supporting Information.[54] After the as-prepared $PSBP_{80}$-*b*-$PNIPAM_{400}$ thin film was probed, 8 mL of D_2O was injected into the reservoir mounted below the thin film to install an unsaturated atmosphere (relative humidity, RH = 85%). The temperature was thermostated at 20 °C by a thermal bath (Julabo F12 MC, Julabo Labor Technology Co. Ltd., Seelbach, Germany). After the hydration of the as-prepared $PSBP_{80}$-*b*-$PNIPAM_{400}$ thin film reached an equilibrium state, the temperature was rapidly increased from 20 °C to 40 °C (first thermal stimulus) and subsequently further increased from 40 °C to 80 °C (second thermal stimulus). The heating rate was around 6 °C min^{-1}.[44] Therefore, the two heating steps took 3.5 and 6.5 min, respectively. The hydration kinetics and response to the thermal stimuli were tracked by in situ NR with a time resolution of 5 s. The obtained NR curves were analyzed by the Motofit package (Andrew Nelson, Australian Nuclear Science and Technology Organization) running within the IGOR Pro software (WaveMetrics, Inc.).[55] SLDs of Si, SiO_2, D_2O, and PNIPAM were fixed at 2.07×10^{-6}, 3.47×10^{-6} , 6.36×10^{-6}, 0.84×10^{-6}, and 0.68×10^{-6} $Å^{-2}$, in accordance with the literature.[37,44] For PSBP, the SLD was calculated from the mass density and monomer structure, assuming a density of 1.0 g cm^{-3}, which was used to characterize the monomer with similar structure in our previous work.[56] By varying the number of layers in the profile of the $PSBP_{80}$-*b*-$PNIPAM_{400}$ thin film and adjusting their thickness, roughness, and SLD value, the evolution of the film structure and kinetics of water transfer was successfully resolved during the hydration and after the thermal stimuli. In our present investigation, the work is mainly focused on tracing the water absorption and transfer upon heating. For this reason, the kinetics of vertical structure and water distribution in the film is of great importance. Both of them can be well observed by the in situ NR measurements whereas optical or atomic force microscopy would only probe the surface structure.

Statistical Analysis: NR data were processed as described in the Supporting Information and data are presented in the format mean ± SD.

Supporting Information

Supporting Information is available from the Wiley Online Library or from the author.

Acknowledgements

N.H. and L.L. contributed equally to this work. This work was supported by the National Natural Science Foundation of China (Grant Nos. 52173087, 51403186, and 51611130312), Zhejiang Provincial Natural Science Foundation of China (LY21E030022), National Key R&D Program of China (2017YFB0309600), the Fundamental Research Funds of Zhejiang Sci-Tech University (Grant No. 2021Y003), and the Deutsche Forschungsgemeinschaft (DFG, German Research Foundation) (PA 771/14-1, MU 1487/17-1, and LA 611/11-1). This work was based upon experiments performed at the D17 at the ILL, Grenoble, France. The authors acknowledge beamtime allocation and excellent equipment.

Correction added on 12 December 2022, after first online publication: Projekt Deal funding statement has been added.

Open access funding enabled and organized by Projekt DEAL.

Conflict of Interest

The authors declare no conflict of interest.

Data Availability Statement

The data that support the findings of this study are available from the corresponding author upon reasonable request.

Keywords

block copolymer, dual thermoresponsive, kinetic water transfer, neutron reflectivity, thin film

Received: August 29, 2022
Revised: October 18, 2022
Published online: December 4, 2022

[1] M. A. Ward, T. K. Georgiou, *Polymers* **2011**, *3*, 1215.
[2] G. Pasparakis, M. Vamvakaki, *Polym. Chem.* **2011**, *2*, 1234.
[3] S. C. Song, S. B. Lee, J. I. Jin, Y. S. Sohn, *Macromolecules* **1999**, *32*, 2188.
[4] A. Halperin, M. Kroger, F. M. Winnik, *Chem., Int. Ed. Engl.* **2015**, *54*, 15342.
[5] F. D. Jochum, P. Theato, *Chem. Soc. Rev.* **2013**, *42*, 7468.
[6] M. I. Gibson, R. K. O'Reilly, *Chem. Soc. Rev.* **2013**, *42*, 7204.
[7] Č. Koňák, T. Reschel, D. Oupický, K. Ulbrich, *Langmuir* **2002**, *18*, 8217.
[8] J. Niskanen, H. Tenhu, *Polym. Chem.* **2017**, *8*, 220.
[9] Y. Kotsuchibashi, M. Ebara, T. Aoyagi, R. Narain, *Polymers* **2016**, *8*, 380.
[10] S. Paschke, K. Lienkamp, *ACS Appl. Polym. Mater.* **2020**, *2*, 129.
[11] A. Laschewsky, A. Rosenhahn, *Langmuir* **2019**, *35*, 1056.
[12] M. C. Sin, S. H. Chen, Y. Chang, *Polym. J.* **2014**, *46*, 436.
[13] S. L. West, J. P. Salvage, E. J. Lobb, S. P. Armes, N. C. Billingham, A. L. Lewis, G. W. Hanlon, A. W. Lloyd, *Biomaterials* **2004**, *25*, 1195.
[14] A. Laschewsky, *Polymers* **2014**, *6*, 1544.
[15] M. Sponchioni, P. R. Bassam, D. Moscatelli, P. Arosio, U. C. Palmiero, *Nanoscale* **2019**, *11*, 16582.
[16] Y. J. Shih, Y. Chang, A. Deratani, D. Quemener, *Biomacromolecules* **2012**, *13*, 2849.
[17] Y. L. Liu, C. Z. Zhao, C. Y. Chen, *Macromolecules* **2022**, *55*, 3801.
[18] F. Zaccarian, M. Baker, M. Webber, *Org. Mater.* **2020**, *2*, 342.
[19] S. Gao, J. Su, W. Wang, J. Fu, H. A. O. Wang, *Cellulose* **2021**, *28*, 1139.
[20] V. Hildebrand, A. Laschewsky, E. Wischerhoff, *Polym. Chem.* **2016**, *7*, 731.
[21] V. Hildebrand, A. Laschewsky, M. Päch, P. Müller-Buschbaum, C. M. Papadakis, *Polym. Chem.* **2017**, *8*, 310.
[22] E. Schönemann, J. Koc, N. Aldred, A. S. Clare, A. Laschewsky, A. Rosenhahn, E. Wischerhoff, *Macromol. Rapid Commun.* **2020**, *41*, 1900447.
[23] E. M. Lewoczko, N. Wang, C. E. Lundberg, M. T. Kelly, E. W. Kent, T. Wu, M. L. Chen, J. H. Wang, B. Zhao, *ACS Appl. Polym. Mater.* **2021**, *3*, 867.
[24] Y. Zhu, J. M. Noy, A. B. Lowe, P. J. Roth, *Polym. Chem.* **2015**, *6*,5705.
[25] T. Wang, R. Kou, H. Liu, L. Liu, G. Zhang, G. Liu, *Langmuir* **2016**, *32*, 2698.
[26] V. Monroy, J. C. Galin, *Polymer* **1984**, *25*, 254.
[27] T. Sakamaki, Y. Inutsuka, K. Igata, K. Higaki, N. L. Yamada, Y. Higaki, A. Takahara, *Langmuir* **2019**, *35*, 1583.
[28] Y. Kotsuchibashi, *Polym. J.* **2020**, *52*, 681.
[29] C. M. Papadakis, P. Müller-Buschbaum, A. Laschewsky, *Langmuir* **2019**, *35*, 9660.
[30] N. S. Vishnevetskaya, V. Hildebrand, N. M. Nizardo, C. H. Ko, Z. Y. Di, A. Radulescu, L. C. Barnsley, P. Müller-Buschbaum, A. Laschewsky, C. M. Papadakis, *Langmuir* **2019**, *35*, 6441.
[31] J. Yin, J. Hu, G. Zhang, S. Liu, *Langmuir* **2014**, *30*, 2551.
[32] N. M. Nizardo, D. Schanzenbach, E. Schonemann, A. Laschewsky, *Polymers* **2018**, *10*, 325.
[33] J. Virtanen, M. Arotçaréna, B. Heise, S. Ishaya, A. Laschewsky, H. Tenhu, *Langmuir* **2002**, *18*, 5360.
[34] L. P. Kreuzer, T. Widmann, L. Bießmann, N. Hohn, J. Pantle, R. Märkl, J. F. Moulin, V. Hildebrand, A. Laschewsky, C. M. Papadakis, P. Müller-Buschbaum, *Macromolecules* **2020**, *53*, 2841.
[35] L. P. Kreuzer, C. Geiger, T. Widmann, P. Wang, R. Cubitt, V. Hildebrand, A. Laschewsky, C. M. Papadakis, P. Müller-Buschbaum, *Macromolecules* **2021**, *54*, 7147.
[36] L. P. Kreuzer, T. Widmann, C. Geiger, P. Wang, A. Vagias, J. E. Heger, M. Haese, V. Hildebrand, A. Laschewsky, C. M. Papadakis, P. Müller-Buschbaum, *Langmuir* **2021**, *37*, 9179.
[37] Q. Zhong, N. Hu, L. Mi, J. P. Wang, E. Metwalli, L. Bießmann, C. Herold, J. Yang, G. P. Wu, Z. K. Xu, R. Cubitt, P. Müller-Buschbaum, *Langmuir* **2020**, *36*, 6228.
[38] H. Sun, X. Chen, X. Han, H. Liu, *Langmuir* **2017**, *33*, 2646.
[39] S. M. Mirvakili, I. W. Hunter, *Adv. Mater.* **2017**, *30*, 1704407.
[40] J. Hu, S. Liu, *Macromolecules* **2010**, *43*, 8315.
[41] M. Karimi, P. S. Zangabad, A. Ghasemi, M. Amiri, M. Bahrami, H. Malekzad, H. Ghahramanzadeh Asl, Z. Mahdieh, M. Bozorgomid, A. Ghasemi, M. R. Rahmani Taji Boyuk, M. R. Hamblin, *ACS Appl. Mater. Interfaces* **2016**, *8*, 21107.
[42] C. Xing, Z. K. Shi, J. L. Tian, J. Sun, Z. B. Li, *Biomacromolecules* **2018**, *19*, 2109.
[43] L. Lei, W. Wang, C. Wang, H. Q. Fan, A. K. Yadav, N. Hu, Q. Zhong, P. Müller-Buschbaum, *J. Mater. Chem. A* **2020**, *8*, 23812.
[44] S. Nieuwenhuis, Q. Zhong, E. Metwalli, L. Biessmann, M. Philipp, A. Miasnikova, A. Laschewsky, C. M. Papadakis, R. Cubitt, J. Wang, P. Müller-Buschbaum, *Langmuir* **2019**, *35*, 7691.
[45] P. Müller-Buschbaum, *Anal. Bioanal. Chem.* **2003**, *376*, 3.
[46] L. P. Kreuzer, T. Widmann, N. Aldosari, L. Bießmann, G. Mangiapia, V. Hildebrand, A. Laschewsky, C. M. Papadakis, P. Müller-Buschbaum, *Macromolecules* **2020**, *53*, 9108.
[47] Q. Zhong, E. Metwalli, M. Rawolle, G. Kaune, A. M. Bivigou-Koumba, A. Laschewsky, C. M. Papadakis, R. Cubitt, P. Müller-Buschbaum, *Macromolecules* **2013**, *46*, 4069.
[48] Q. Zhong, E. Metwalli, G. Kaune, M. Rawolle, A. M. Bivigou-Koumba, A. Laschewsky, C. M. Papadakis, R. Cubitt, P. Müller-Buschbaum, *Soft Matter* **2012**, *8*, 5241.
[49] Y. Li, T. Tanaka, *J. Chem. Phys.* **1990**, *92*, 1365.
[50] N. Hu, L. Mi, E. Metwalli, L. Bießmann, C. Herold, R. Cubitt, Q. Zhong, P. Müller-Buschbaum, *Langmuir* **2022**, *38*, 8094.
[51] T. J. Murdoch, B. A. Humphreys, E. C. Johnson, S. W. Prescott, A. Nelson, E. J. Wanless, G. B. Webber, *Polymer* **2018**, *138*, 229.
[52] K. Haraguchi, J. Ning, G. Li, *Eur. Polym. J.* **2015**, *68*, 630.
[53] N. S. Vishnevetskaya, V. Hildebrand, M. A. Dyakonova, B. J. Niebuur, K. Kyriakos, K. N. Raftopoulos, Z. Di, P. Müller-Buschbaum, A. Laschewsky, C. M. Papadakis, *Macromolecules* **2018**, *51*, 2604.
[54] G. M. Su, I. A. Cordova, M. A. Brady, D. Prendergast, C. Wang, *Polymer* **2016**, *99*, 782.
[55] A. Nelson, *J. Appl. Crystallogr.* **2006**, *39*, 273.
[56] N. S. Vishnevetskaya, V. Hildebrand, B. J. Niebuur, I. Grillo, S. K. Filippov, A. Laschewsky, P. Müller-Buschbaum, C. M. Papadakis, *Macromolecules* **2017**, *50*, 3985.